

# On the Modelling of Zero Impedance Branches for Power Flow Analysis

Federico Milano, *Senior Member, IEEE*

**Abstract**—This letter compares three models of zero impedance branches for power system analysis and proposes a new, simple yet reliable model of such a component based on a steady-state droop control approach. The proposed model proves to be numerically robust and allows representing both short lines as well as the internal electrical nodes that compose substations. Parallel and lossy zero impedance branches can also be straightforwardly defined. A detailed discussion of the features and numerical performance of all models considered in this letter is carried out by means of the a 21,177-bus model of the European ENTSO-E transmission.

**Index Terms**—Zero impedance branch, admittance matrix, power flow analysis.

## I. POWER FLOW MODELS OF ZERO IMPEDANCE BRANCHES

THE problem of the modelling of zero or small impedance branches arises in power flow analysis [1] and state estimation [2]. While zero impedance branches are often neglected and collapsed into a unique node, structural changes that power systems are undergoing in the last decade and the increasing interaction between transmission and distribution systems stress the need for an accurate modelling of every aspect of the power grid. Switching branches within a substation and short transmission lines connecting, for example, networks with different owners, are among these.

This letter focuses on the modelling of zero impedance branches for power flow analysis. This section presents a taxonomy of the models available in the literature as well as the proposed model based on power injections and a steady-state droop control approach.

### Model A – Small Impedance Model

The conventional approach to model of zero impedance branches is based on approximating the the connection using a *small* impedance  $j\epsilon_x$  (see Fig. 1.a) and including such impedance into the network admittance matrix [1]. The resulting active and reactive power injections of the branch are thus dependent on the inverse of  $\epsilon_x$ . For example, the injections at bus  $h$  are:

$$\begin{aligned} p_h &= \frac{v_h v_k}{\epsilon_x} \sin(\theta_h - \theta_k) && \propto \frac{1}{\epsilon_x} \\ q_h &= \frac{v_h^2}{\epsilon_x} - \frac{v_h v_k}{\epsilon_x} \cos(\theta_h - \theta_k) && \propto \frac{1}{\epsilon_x} \end{aligned} \quad (1)$$

The expression for  $p_k$  and  $q_k$  can be obtained from (1) by swapping  $h$  and  $k$  subindices. Due to the dependency on the inverse of  $\epsilon_x$ , this approach shows intrinsic numerical instabilities, e.g., collinearity, as small impedance values increase the condition number of the power flow Jacobian matrix and to lead to ill-conditioned cases.

### Model B – Two Fictitious Reactance Model

Another approach consists in using a series of two fictitious impedances with equal magnitude but opposite sign [3]. This solution introduces also an additional fictitious bus per each zero impedance branch, as shown in Fig. 1.b. Recently, a similar approach but applied to small-impedance distribution transformers has been discussed in [4] and other papers by the same first author cited therein. The power injections at the fictitious bus are:

$$\begin{aligned} 0 = p_i &= \frac{v_i v_h}{x} \sin(\theta_i - \theta_h) - \frac{v_i v_k}{x} \sin(\theta_i - \theta_k) \\ 0 = q_i &= -\frac{v_i v_h}{x} \cos(\theta_i - \theta_h) + \frac{v_i v_k}{x} \cos(\theta_i - \theta_k) \end{aligned} \quad (2)$$

Manuscript submitted to PES Letters, July 2015.

F. Milano is with School of Electrical and Electronic Engineering, University College Dublin, Ireland. E-mail: federico.milano@ucd.ie

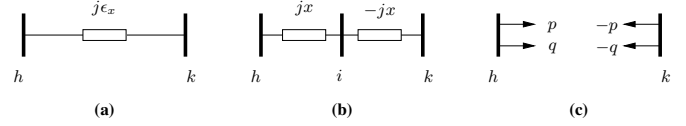


Fig. 1. Different models of zero impedance branches: (a) small reactance  $j\epsilon_x$ ; (b) series of two reactances  $jx$  and  $-jx$ ; and (c) power injection model.

and, after simplifying common terms:

$$\begin{aligned} 0 &= v_h \sin(\theta_i - \theta_h) - v_k \sin(\theta_i - \theta_k) \\ 0 &= v_h \cos(\theta_i - \theta_h) - v_k \cos(\theta_i - \theta_k) \end{aligned} \quad (3)$$

Note that, while  $\theta_h = \theta_k$  and  $v_h = v_k$  is a solution of (2) and (3), this solution is not unique as (2) and (3) as well as the expression of the active and reactive power injections at buses  $h$  and  $k$ , are nonlinear. Moreover, to provide a feasible solution, the power flow across the branch must satisfy the condition  $|p_h| < p_h^{\max} = v_h v_i / x$ .

### Model C – Short-circuit Power Injection Model

A conceptually different approach can be found in works related to state estimation. Pioneering work has been done in [2] and [5]. Then, based on the aforementioned references, a zero impedance model for power flow analysis is proposed in [6]. This model defines two short-circuit constraints:

$$0 = \theta_h - \theta_k, \quad 0 = v_h - v_k \quad (4)$$

and active and reactive power injections at nodes  $h$  and  $k$  through two additional variables, namely,  $p$  and  $q$  (see Fig. 1.c), as follows:

$$p_h = p, \quad p_k = -p, \quad q_h = q, \quad q_k = -q \quad (5)$$

### Model D – Proposed Droop-based Power Injection Model

The proposed model consists in defining power injections at sending and receiving ends, i.e., (5), and two constraints based on a steady-state droop control, as follows:

$$0 = \theta_h - \theta_k - d_p p, \quad 0 = v_h - v_k - d_q q \quad (6)$$

where  $d_p$  and  $d_q$  are small positive coefficients whose effect is similar to that of steady-state droop controllers. The terms  $d_p p$  and  $d_q q$  introduce, in fact, a negative-slope mismatch of the voltage phasors of nodes  $h$  and  $k$ . Note that, if  $d_p = d_q = 0$ , (6) reduce to (4). Model C above is a particular case of the proposed model.

The proposed model shows some advantages with respect to the previous models, as discussed below and summarized in Table I.

1) *Linearity*: Equations (5) and (6) are linear and, hence, Model D can be expected to be numerically robust (see the case study below). Model C is also linear, while Models A and B are not. It can be useful to note that Model D is **not** a linearization of Model A but, rather, a generalization of Model C, which is formally equivalent to a steady-state integral controller.

2) *Parallel branches*: Parallel zero-impedance branches can be modelled without any additional effort as the coefficients  $d_p$  and  $d_q$  unequivocally define the distribution of power flows in the parallel branches. Equations (6), in fact, are both formally similar to a resistive dipole where the droop coefficients  $d_p$  and  $d_q$  are the fictitious resistances. Parallel branches can be also implemented using Model A and B, but not Model C. In Model C, in fact, each

TABLE I  
FEATURES OF ZERO IMPEDANCE MODELS

Model	Variables	Linearity	Parallel Branches	Losses
A	–	no	yes	yes
B	$v_i, \theta_i$	no	yes	yes
C	$p, q$	yes	no	no
D	$p, q$	yes	yes	yes

parallel branch introduces two sets of (5), with two unknowns each, but only one set of (4) can be defined. Hence, the powers flowing in parallel branches are undetermined if Model C is used.

3) *Losses*: While Models A and B can straightforwardly include losses, Model C cannot. In Model D, losses can be implicitly taken into account through the coefficients  $d_p$  and  $d_q$ , as follows. From (1) and assuming  $v_h^2 \approx v_h$ ,  $v_h v_k \cos(\theta_h - \theta_k) \approx v_k$ , and  $v_h v_k \sin(\theta_h - \theta_k) \approx \theta_h - \theta_k$ , one obtains  $d_p \approx d_q \approx \epsilon_x$ . In the same vein, considering the detailed power flow equations and assuming that the connection is characterized by a series impedance  $r + jx$ :

$$p_h = v_h^2 g - v_h v_k (g \cos(\theta_h - \theta_k) + b \sin(\theta_h - \theta_k)) \quad (7)$$

$$q_h = -v_h^2 b - v_h v_k (g \sin(\theta_h - \theta_k) - b \cos(\theta_h - \theta_k))$$

and applying same approximations as above, active power losses could be also approximated by means of the following expression:

$$0 = \theta_h - \theta_k - \epsilon_x p - \epsilon_r q \quad (8)$$

$$0 = v_h - v_k - \epsilon_x q + \epsilon_r p$$

where  $g + jb = (r + jx)^{-1}$ , and  $\epsilon_x = \frac{-b}{g^2 + b^2}$  and  $\epsilon_r = \frac{-g}{g^2 + b^2}$ .

## II. CASE STUDY

In this case study, the properties and the performance of the four zero impedance models discussed in the previous section are compared through a steady-state model of the ENTSO-E transmission system.<sup>1</sup> The model includes 21,177 buses, 30,968 transmission lines and transformers, 1,144 zero impedance branches, 15,756 loads, and 4,828 generators.

All simulations are obtained using a standard polar-coordinate flat-start Newton method implemented in Dome [7]. The convergence tolerance used in the case study is  $\epsilon = 10^{-6}$ . The Dome version used for in this case study is based on Python 3.4.1, ATLAS 3.10.1, CVXOPT 1.1.7, and KLU 1.3.2. Simulations were executed on a 64-bit Linux Fedora 21 operating system running on a Intel i7 2.10 GHz CPU, and 8 GB of RAM. CPU times shown in the remainder of this section are computed as the average over ten simulations.

Results of the power flow analysis for the ENTSO-E transmission system and considering all zero impedance models are shown in Table II. As expected, Model A shows numerical issues if the value of the branch impedance is too small. In particular, divergence occurs for  $\epsilon_x \leq 10^{-10}$ . The value at which divergence occurs depends on several factors, for example, the topology of the system and the computer representation of floating point numbers. Reference [1] provides a method to define the minimum value of the impedance that allows obtaining a solution with the Newton algorithm.

Two variants of Model B are considered. Model B.1 consists in a bus and two lines with impedance  $jx$  and  $-jx$ , respectively. This model increases the number of buses and connections. For example, considering this model, the ENTSO-E system contains 22,321 buses and a total of 33,256 branches. To avoid the system size increase, which can slow down the power flow analysis, an alternative Model B.2 is considered and is obtained by embedding (3) in a custom branch model. Model B.2 defines two variables, namely  $v_i$  and  $\theta_i$ , but no additional buses or lines are required and hence it can be useful whenever it is needed to preserve the original topology of the network. Table II shows results for Models B.1 and B.2 for a

<sup>1</sup>The data of the system has been licensed to the author by ENTSO-E. Data can be requested through an on-line application at [www.entsoe.eu](http://www.entsoe.eu).

TABLE II  
COMPARISON OF THE PERFORMANCE OF ZERO IMPEDANCE MODELS

Model	Parameters	Iterations	CPU time [s]
A	$\epsilon_x = 10^{-8}$ pu	7	0.3650
A	$\epsilon_x = 10^{-9}$ pu	9	0.4418
A	$\epsilon_x = 10^{-10}$ pu	diverges	–
B.1	$x = 0.1$ pu	7	0.3656
B.1	$x = 1.00$ pu	8	0.4023
B.1	$x = 2.00$ pu	13	0.6272
B.2	$x = 0.1$ pu	7	0.3501
B.2	$x = 1.00$ pu	13	0.6077
B.2	$x = 2.00$ pu	11	0.5321
C	$d_p = d_q = 0$	7	0.3578
D	$d_p = d_q = 10^{-8}$	7	0.3441
D	$d_p = d_q = 10^{-12}$	7	0.3434
D	$d_p = d_q = 10^{-18}$	7	0.3360

TABLE III  
COMPARISON OF THE PERFORMANCE OF ZERO IMPEDANCE MODELS WITH INCLUSION OF PARALLEL ZERO IMPEDANCE CONNECTIONS

Model	Parameters	Iterations	CPU time [s]
A	$\epsilon_x = 10^{-8}$ pu	7	0.3630
B.1	$x = 0.1$ pu	7	0.3608
B.2	$x = 0.1$ pu	39	1.7760
C	$d_p = d_q = 0$	diverges	–
D	$d_p = d_q = 10^{-8}$	7	0.3475

typical value of the branch reactance, i.e.,  $x = 0.1$  pu, as well as for higher values, i.e.,  $x = 1$  and  $x = 2$  pu, which are aimed to emulate congestion. As it can be observed, these models show similar numerical issues as  $|p_h|$  approaches  $p_h^{\max}$ . Note also that the extra computational burden introduced by Model B.1 has a small effect on CPU times. Finally, Table II shows that the performance and the computational burden of Models C and D are similar, as expected. Note that a sufficient condition to obtain an accurate solution through Model D is that  $d_p \ll \epsilon$  and  $d_q \ll \epsilon$ . Note also that  $d_p$  and  $d_q$  must not need to be equal.

A second test is carried out by including a small number, i.e., about 1% of the total, of parallel zero impedance connections. Results obtained with the models discussed in this letter are shown in Table III. As expected, Model C diverges, as parallel connections lead to an underdetermined set of equations. Also Model B.2 shows numerical difficulties. While it converges, the solution is reached after several iterations during which the maximum mismatch shows an erratic behaviour before decreasing quadratically as expected in a Newton method.

## REFERENCES

- [1] D. J. Tylavsky, P. E. Crouch, L. F. Jarriel, J. Singh, and R. Adapa, "The Effect of Precision and Small Impedance Branches on Power Flow Robustness," *IEEE Trans. on Power Systems*, vol. 9, no. 1, pp. 6–14, Feb. 1994.
- [2] A. Monticelli and A. Garcia, "Modeling Zero Impedance Branches in Power System State Estimation," *IEEE Trans. on Power Systems*, vol. 6, no. 4, pp. 1561–1570, Nov. 1991.
- [3] A. A. Mazi, B. F. Wollenberg, and M. H. Hesse, "Corrective Control of Power System Flows by Line and Bus-Bar Switching," *IEEE Trans. on Power Systems*, vol. 1, no. 3, pp. 258–264, Aug. 1986.
- [4] Y. Yao, C. Wang, X. Jiang, and C. Wang, "Small Impedance Branches on Convergence of the Newton Power Flow in Rectangular Form," in *Int. Conf. on Power Electronics and Intelligent Transportation System*, vol. 2, Dec. 2009, pp. 6–9.
- [5] A. Monticelli, "The Impact of Modelling Short Circuit Branches in State Estimation," *IEEE Trans. on Power Systems*, vol. 8, no. 1, pp. 364–370, Feb. 1993.
- [6] E. M. Lourenço, N. S. da Silva, and A. S. Costa, "Fast Decoupled Steady-State Solution for Power Networks Modeled at the Bus Section Level," in *Procs. of the IEEE Bucharest Power Tech Conference*, Bucharest, Romania, July 2009.
- [7] F. Milano, "A Python-based Software Tool for Power System Analysis," in *Procs. of the IEEE PES General Meeting*, Vancouver, BC, July 2013.